INSTITUTE OF PHYSICS PUBLISHING JOURNAL OF PHYSICS D: APPLIED PHYSICS
J. Phys. D: Appl. Phys. **38** (2005) 363–370 doi:10.1088/0022-3727/38/3/002

A read and write element for magnetic probe recording

C B Craus[1], T Onoue, K Ramstöck, W G M A Geerts, M H Siekman, L Abelmann and J C Lodder

Systems and Materials for Information storage (SMI), MESA+, University of Twente, Enschede, The Netherlands

E-mail: c.b.craus@el.utwente.nl

Received 1 August 2004, in final form 29 November 2004
Published 20 January 2005
Online at stacks.iop.org/JPhysD/38/363

Abstract
We present our results on the development of magnetic sensors for application in magnetic probe recording. Successful writing experiments on a magnetic medium with perpendicular anisotropy show that magnetic domains of 130 nm can be reversed in a heat-assisted process. For reading purposes we propose a magnetoresistive sensor. The optimization of the shape of the sensor was performed using micromagnetic simulations with the requirement that the sensor has to be capable of both read and write operations. At this stage, the experimental realization of the sensor was carried out at a wafer-base level. The fabrication technique consists of a combination of optical lithography and focused ion beam etching.

(Some figures in this article are in colour only in the electronic version)

1. Introduction

Due to the widespread use of mobile, hand-held devices, the need for an information storage device with a high storage capacity and small dimensions is an important issue in the high-tech industry. The solutions adopted up to now can be divided into two categories: electrically addressed (flash memories) and mechanically adressed (microdrives). At the moment, the limitations of the systems based on the above-mentioned solutions are a further reduction of the minimum feature size in the lithographical process for Flash and minimum thickness and power consumption for microdrives.

A possible alternative to these solutions would be to use a device based on Micro-Electro-Mechanical System (MEMS) technology. The concept consists in placing a movable two-dimensional probe array above the storage medium. Data storage is performed by mechanical scanning of the probe array or storage medium. This solution would have the great advantage of high density, low power consumption and low access time. Recently, the IBM Zürich research laboratory demonstrated the principle of parallel probe array storage by using heated cantilever tips and beams and a polymer thin film as a storage medium [1]. Alternatively, a magnetic medium can be considered. The reasons would be: (i) magnetic recording is a proven technology, (ii) infinite erasability of the storage medium, (iii) low power consumption and (iv) the sensors developed for parallel probe arrays can be used in other disciplines like (magnetic) scanning probe microscopy (SPM).

In figure 1 we present the read and write principle for a magnetoresistive sensor as one unit of the probe array. Reading can be performed by measuring the change in resistance of the probe when scanning the magnetic bits. This operation has to be performed in such conditions that the probe does not permanently disturb the local distribution of the magnetization. The same probe can be used for writing/erasing information by using the tip locally to concentrate an external magnetic

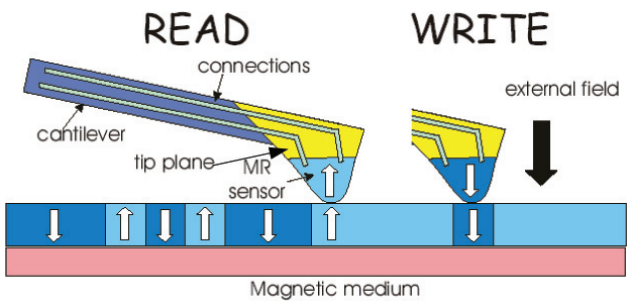

Figure 1. Reading and writing with a magnetoresistive probe.

[1] Author to whom any correspondence should be addressed.

Table 1. Writing modes for a magnetic medium; the probe is in contact with the medium. The quantities are explained in the text.

Mode	Probe	Probe function	Temperature of reversal	Local switching field
W1	Magnetic	Increases the local field	Room temperature	$H_{R1} = H_{ex} + H_{tip} \approx H_C$
W2	Conducting and nonmagnetic	Local heating	Close to T_C	$H_{R2} = H_{ex} < H_C$
W3	Conducting and magnetic	Local heating and increases the local field	Close to T_C	$H_{R3} = H_{ex} + H_{tip} < H_C$

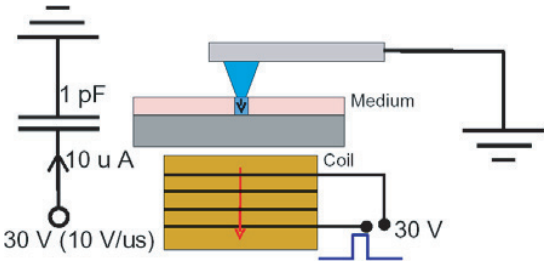

Figure 2. Magnetic probe writing set-up; the equivalent circuit is presented on the left-hand side.

field. In this paper, we present our results on the realization of magnetic probes that can be integrated in a probe array memory. In section 2 we give a brief description of the writing principles and present our writing experiments in combination with media development. Section 3 is reserved for the reading probe. To determine the optimum shape of the probe, we have used micromagnetic simulations. In this design we have taken into account that besides reading, the probe has to be suitable for writing as well. The experimental investigations, at this stage, were carried out on wafer based structures. Conclusions and recommendations for the integration of the probe on a cantilever are given in the last section.

2. Probe writing on magnetic medium

In our approach, we use a magnetic medium with strong perpendicular anisotropy. In the ideal case the medium has a coercivity determined by uniformly localized pinning centres, i.e. there are no local variations of the coercivity on a large spatial scale. This is an important prerequisite because the coercivity of the medium H_C determines the required strength of the local external field H_R (the writing field). Additionally, if the density of the pinning centres is not high enough (with a spatial correlation much larger than the probe radius), the induced transitions will have a large range of dimensions, leading to an increase of noise.

There are multiple choices for the writing process, depending on the type of reversal principle involved. The conditions under which magnetization reversal can take place are summarized in table 1. We take the coercive field of the medium H_C, measured at room temperature, as the reference against which the local switching fields $H_{Ri\ (i=1,3)}$ for each mode are compared. Because an external field H_{ex} is required, a coil is placed in the proximity of the magnetic medium as depicted in figure 2.

In the first mode (W1), the local magnetization reversal is induced by applying a local field $H_{R1} = H_{ex} + H_{tip}$ exceeding the coercive field; H_{tip} represents the stray field provided by the magnetic tip. H_{R1} can be controlled by adjusting the tip–medium distance and the magnetization orientation of the tip via H_{ex}. In the second mode (W2) a short, high-pulsed current can be applied between the probe and the medium. This current causes local heating, and when the medium temperature is close to the Curie temperature T_C the coercivity is lowered. The magnetization in the heated volume reverses due to the strong demagnetizing field from the surrounding material, like in magneto-optical recording [2]. These types of experiments were performed in the past on continuous media. In this writing mode, sharp STM tips can be used with the advantage of a tip radius down to 10 nm and, consequently, comparable reversed volumes for a suitable medium [3]. Erasure of single written bits with this STM method seems to be impossible, whereas erasure of a complete area required application of a strong magnetic field capable of saturating the medium. The last mode (W3) is a combination of the first two. We can reverse the magnetization by locally increasing the temperature and concentrating the external field by the magnetic probe. Because the tip is in contact with the medium, problems related to tip positioning are avoided. Erasing in this mode can be performed in a similar way as writing. More details of this technique will be given in the next subsection.

Once we remove the tip from the written region, the reversed magnetic domain will expand or shrink until it encounters a magnetic defect that will stabilize the local magnetic configuration. Usually, the shape of such a volume is cylindrical with a certain radius R. The final value of R depends on the perpendicular anisotropy constant K and the film thickness. This can be explained by the competition between the demagnetizing energy of the initial magnetic domain (expansion effect) and the domain wall energy (constrictive effect). The range $[B1, B2]$ within which such a domain will be stable can be determined from the following relations, as obtained from the bubble theory [4]:

$$H_C = B_1 + B_2, \tag{1}$$

$$B_1 - B_2 = \frac{\sigma - 6\pi t M_S^2}{M_S R}, \tag{2}$$

where B_1 and B_2 are the external field values corresponding to collapse and expansion of the stable magnetic domain, M_S is the saturation magnetization, σ the domain wall energy per unit area and t the thickness of the medium. Equations (1) and (2) are obtained assuming that (i) the exchange coupling between spins is isotropic and is confined to the nearest neighbours and (ii) the domain wall is a simple Bloch wall. In the process of development of a magnetic medium suitable for high storage density one must take all the above-mentioned parameters into consideration.

2.1. Recording experiments

Magnetic probe recording experiments were performed with a commercial MFM (3100, Digital Instruments) equipped with a coil (see figure 2). The coil is connected to a pulse generator with a current amplifier able to deliver current pulses of 40 A, so that short, strong magnetic field pulses can be generated. A CoNi/Pt multilayered sample was positioned above the coil. A magnetic field pulse of 270 μs was applied in a direction opposite to the magnetization direction of the film (which is in the saturated magnetization state). As a result, a local magnetization reversal is initiated just beneath the tip. A Si AFM tip coated on one side with a NiFe or a Co layer was used both for writing as well as for observing the magnetic domain structure by MFM. In principle, the type of magnetic material deposited onto the tip does not affect the size of the written dots since the magnetic element is saturated during the writing process by the external field from the coil.

We have chosen the CoNi/Pt multilayered film recording medium because it shows a squareness ratio (SQR) of 1, high Q factor ($= K - u/K_{\mathrm{d}}$ of 4.6–5, where $K_u = 3.52 \times 10^5\ \mathrm{J\,m^{-3}}$ is the perpendicular magnetic anisotropy constant and K_{d} is the demagnetization energy) and a steep magnetization reversal. These are important conditions for high writing sensitivity [5]. Other relevant parameters of the magnetic medium are a coercive field H_{C} of 146 kA m^{-1} and saturation magnetization $M_{\mathrm{S}} = 350\ \mathrm{kA\,m^{-1}}$. These magnetic properties can be tuned by adjusting the Ar pressure during deposition. Especially for application in probe recording, the so-called 'double layered structure' was used, with which small magnetic domains as well as high writing sensitivity can be achieved. This film is composed of two layers that are deposited with different Ar pressures. The bottom layer, deposited at low pressure, realizes steep magnetization reversal so that it shows high write sensitivity, and the upper layer, deposited at high pressure, induces pinning sites which restrict domain wall propagation [6].

In our recording set-up, electric charging of the coil below the sample (top of the coil) induced an electric current through the tip, which locally heated the sample. Since the CoNi/Pt multilayered medium used in this experiment had a low Curie temperature of approximately 250°C [6], this local heating reduces the coercivity and aids in the nucleation of magnetization rotation. Therefore, the write experiment performed in this work was heat-assisted magnetic probe recording (W3). In this nucleation mechanism, a sharp tip is desirable to obtain higher current density at the top of the tip so that it heats up properly a localized area in the film. A great advantage of probe recording is that the sharp tip helps in achieving high recording resolution as well as enabling the writing of dots on a high coercivity medium. This mechanism also gives a variety of choices for the probe recording media.

Figure 3(a) shows the results of writing an array of reversed domains by this computer-controlled set-up. The domains showed winding domain walls, caused by restricted domain wall propagation due to pinning sites in the film. By optimizing the writing condition, a clear circular magnetic dot was obtained with a diameter of 130 nm (figure 3(b)). Figure 3(c) shows the results of writing two bits close together, separated by a distance of 50 nm. This distance corresponds to a 360° domain wall having a thickness $d = 2\pi\sqrt{A/K}$. Our

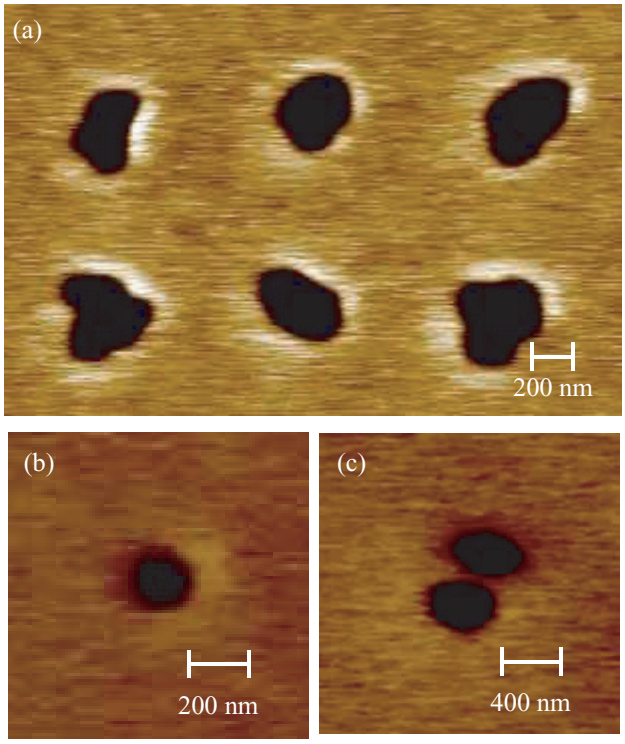

Figure 3. MFM images of (a) an array of written dots, (b) the smallest dot obtained in this experiment and (c) the result of closest dot writing.

results obviously show that it is possible to use the CoNi/Pt medium as a magnetic probe recording medium. From the results shown in figures 3(b) and (c), the achievable recording density is calculated to be 5.1 Gb cm^{-2} (29.4 Gb in^{-2}).

If we consider that our storage medium has a uniform H_{C} and a domain wall energy $\sigma = 4\sqrt{A/K}$, where A is the exchange stiffness constant, then, using equations (1) and (2), we obtain a minimum size of the reversed magnetic domain $2R = 80$ nm, in close agreement with our experimental results. This leads to a theoretical maximum recording density of 57.6 Gb in^{-2}.

3. Magnetoresistive probes

3.1. Element design

Magnetoresistive probes make read and write operations with the same device possible. In this case, a simple rectangular shape of the sensor like in hard disk heads is not desirable. The sensor should be elongated perpendicular to the medium [7], with a sufficiently high aspect ratio (>5) so that a high stray field can be generated. During the writing process the probe will increase the uniform field generated by a coil situated under the magnetic medium in the region where the magnetization has to be reversed (W1 or W3). In order to achieve maximum writing performance the head has to be in contact with the medium. This aspect will be taken into account when the structure is realized on the tip.

In figure 4 the proposed structure is presented. The sensing principle is simply anisotropic magnetoresistance:

$$\rho_{\mathrm{l}} = \rho_0 + \Delta\rho_{\mathrm{l}} \cos^2(\theta), \tag{3}$$

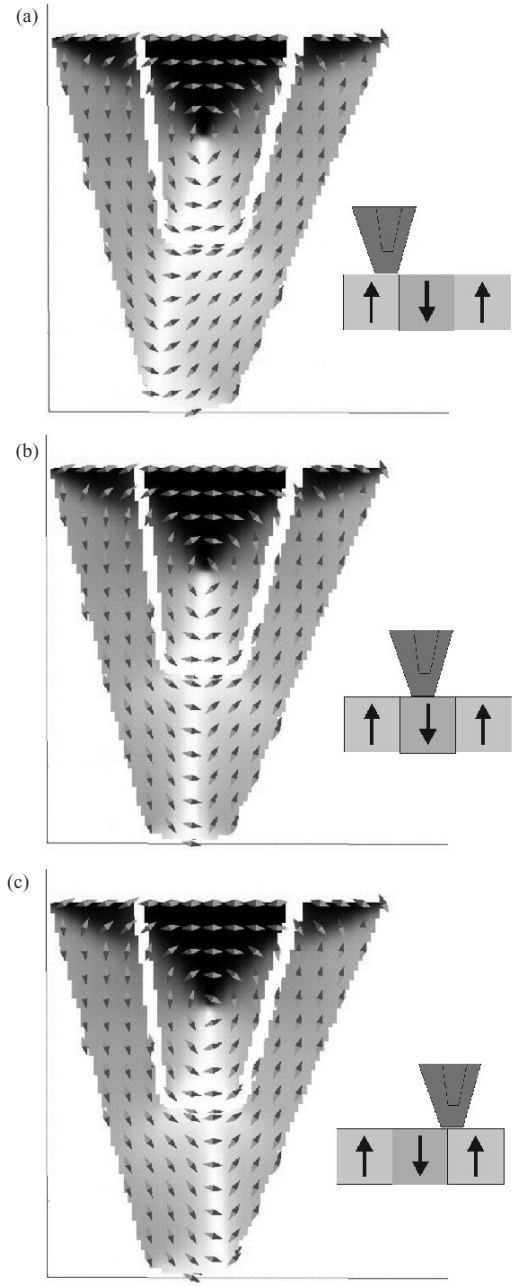

Figure 4. Simulation of the magnetization distribution corresponding to a magnetic element scanning a reversed magnetic domain; the positions are indicated in each image. Dimensions: length 800 nm, upper width 500 nm, lower width 200 nm and thickness 20 nm.

where ρ_l is the local resistivity and θ the angle between the local magnetization and the current direction. The total change in resistance ΔR is given by the overall magnetization distribution and its total resistance. Therefore, the shape plays a major role in designing the sensor. Having this in mind, we have proposed a structure with trenches along the edges (grooves deeper than the thickness of the ferromagnetic layer). The trenches are small, so that the total resistance of the device increases while keeping the magnetization coupled over the entire area of the sensor, as is required for the writing and stability of the domain pattern in the sensor. The current is forced to pass only in the bottom region of the sensor. Additionally, the part of the trench parallel to the medium (in our case perpendicular to the long axis of the sensor) serves to align the local magnetization in the tip as close as possible parallel to the medium. This has two advantages: (i) in the remanence state, the component of the stray field from the probe towards the medium will have minor influence on the stored information and (ii) the response of the sensor is well defined and without hysteretic effects. The sensor shape was optimized so that the bottom region of the sensor has a maximum change in magnetization orientation when scanning over the magnetic medium.

Numerical simulations were carried out, calculating both the current distribution solving the Laplace equations and the magnetization configuration using a large scale finite micromagnetic method [8]. The intrinsic parameters were $M_S = 800 \times 10^3\,\mathrm{A\,m^{-1}}$, $A = 1.05 \times 10^{-11}\,\mathrm{J\,m^{-1}}$, $K_1 = 1.05 \times 10^2\,\mathrm{J\,m^{-3}}$ and a discretization cell size less than 3.75 nm, a value smaller than the estimated exchange length. It turns out that a total MR response when the sensor scans a magnetic transition would be approximately 0.5% of the total resistance. This change is within our measurement possibilities. What is remarkable about this structure is the stability due to the vortex-like magnetic configuration and the fact that in real scanning experiments the structure will need only low field biasing, or none at all. The simulation shows that the magnetization changes its orientation only in the bottom part of the sensor. During scanning, the bright area depicted in figure 4 changes its position from left to right at the bottom part of the sensor. This bright region corresponds to a rotation of the magnetization of approximately 100°. The reverse movement happens when the sensor scans again over regions with magnetization oriented as in the initial situation. Such behaviour promotes a slight skew ($<10°$) in the vertical axis of the probe. The change in magnetoresistance originates from a change in local orientation of the magnetization in combination with the inhomogeneous current distribution at the bottom of the sensor.

3.2. Experimental realization of the MR element

Taking into account the requirements mentioned before, we have fabricated magnetic structures using a combination of standard optical lithography and focused ion beam (FIB) etching. Details regarding FIB etching and ion implantation of Permalloy layers can be found in [9]. We have tried to simplify the fabrication procedure by performing the experiments on a wafer rather than a cantilever, because a wafer based approach give us a larger freedom in testing magnetic structures and because the electrical wiring on the cantilevers is an issue that has to be solved separately. For mask design a parameter-based design package was used, which enables modifications to be made easily.

The first step in the fabrication procedure is to create a 500 nm SiO layer by wet oxidation (5 min at 1100°C). The MR elements (70 nm thick) and the aluminium electrodes (500 nm thick) are defined by conventional lithography and ultrasonic-assisted lift-off. We did not apply any post-backing treatment after development of the negative photo-resist. The magnetic Permalloy ($Ni_{80}Fe_{20}$) film for the MR sensor was deposited by evaporation or RF sputter deposition.

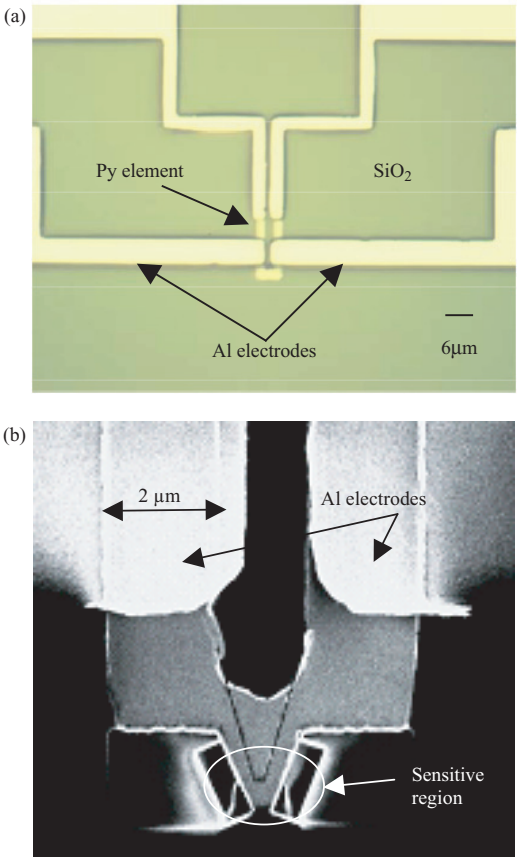

Figure 5. (*a*) MR element with Al electrodes obtained by optical lithography. (*b*) SEM image of the structure obtained after FIB etching.

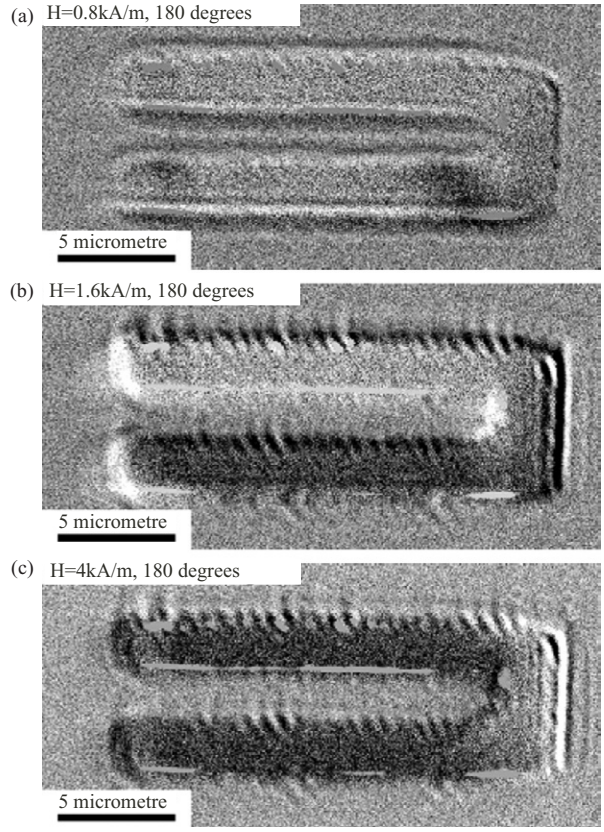

Figure 6. Kerr measurements showing the switching mechanism of the U-shaped elements. The values of the external field applied along the legs are included.

DC hysteresis loops measured for both types of films show soft magnetic characteristics with a coercive field and induced anisotropy below $0.4\,\mathrm{kA\,m^{-1}}$. A light microscopy picture of a typical MR element with four Al electrodes for resistivity measurements is presented in figure 5(*a*). In figure 5(*b*) we present the structures obtained after FIB etching. In this way, we obtain the MR response mainly from the bottom area. Although the structure is much larger than the one we propose in the previous section, the sensitive area of the sensor has a similar shape, including the trenches for electrical isolation and induced magnetic anisotropy. Since the voltage electrodes are situated at 4 μm from the bottom of the element, a contribution of the leg resistance is expected to appear in the MR measurements performed in dc magnetic field. Apart from this, coupling of the magnetization in the bottom of the sensor with the magnetization in the vertical legs will play a role. This could also give indirect information on the magnetization behaviour in the nonuniform field of the magnetic medium. Therefore, the first step in our approach is to understand the magnetization reversal of the structure obtained after optical lithography patterning. We focus on the switching mechanism of the legs and its influence on the MR response and then we discuss the magnetoresistance behaviour of the FIB-etched structure. The characterization techniques were magnetic force microscopy, scanning electron microscopy (SEM) and in-plane Kerr microscopy. The magnetoresistance was measured using a SR830 DSP lock-in amplifier with a computer interface. A current density $J < 5 \times 10^6\,\mathrm{A\,cm^{-2}}$ was chosen such that damaging of the sensor due to electromigration effects [10] was avoided.

The best tool in investigating the magnetization distribution as a function of the external field, corresponding to structures with micrometre-sized dimensions, is in-plane Kerr microscopy. In our case, this structure is a U-shaped patterned element. Our Kerr set-up has a resolution of approximately 500 nm; therefore, smaller magnetization distributions (especially those of the FIB-ed structures) cannot be observed. A much better resolution is obtained with our magnetic force microscope [11], but in the instrument used no external fields could be applied. All these measurements will be used to explain the magnetoresistance response of this structure.

The Kerr images presented in figure 6 were obtained by subtraction from a reference image; the applied field was oriented along the legs. We first saturate the sample at $H_{\mathrm{ext}} = -80\,\mathrm{kA\,m^{-1}}$ and then take the reference image at $H_{\mathrm{ext}} = -8\,\mathrm{kA\,m^{-1}}$. It is clear that the switching takes place in an interval of approximately $\Delta H_{\mathrm{ext}} = 2.4\,\mathrm{kA\,m^{-1}}$. In figure 6(*a*) weak magnetic contrast can be observed in the lower leg. This can be due to pinning of the domain walls. The magnetization reversal mechanism can be complicated, being composed of both spin rotation and domain wall propagation. The pinning centres can be the rims of the structure, caused by the fact that the deposition of Permalloy is not highly directional and the cross section of the resist-covered surface after the

development procedure does not have the desired rectangular shape. Due to the small distance between the legs (only 2 μm), a relatively strong stray field interaction is expected. This was shown for stripe-patterned Permalloy structures [12], where the magnetic domains were not influenced by separations below 30 μm. Our samples, however, have different shapes and different thicknesses, as compared with those used in the above-mentioned paper, so we cannot directly compare our Kerr measurements. Additionally, the simulations (not shown here) of much smaller U-shaped sensors with a length of approximately 2 μm, but with a similar shape, reveal that the legs switch at two different values. Because the simulated structures were smaller than the ones produced by optical lithography, the switching fields were quite large (around 24 kA m^{-1}).

When H_{ext} was applied perpendicular to the legs no independent switching was observed. This may prove that in these conditions the reversal of the magnetization process is different. Such a hypothesis was also confirmed by MR measurements (not shown here). However, because these magnetic elements are supposed to be used when the stray field from the magnetic medium is oriented along the sensor, this situation is less important.

The DC-MR measurement of the sensor before FIB etching is presented in figure 7(*a*). We observe that the overall shape of the plot is specific for the situation when the magnetization rotates from $\theta_{\mathrm{initial}} > \theta_{\mathrm{final}}$. The relative change in resistance is less than 2% as expected for Permalloy thin films because (i) the current distribution is not homogeneous and (ii) at the remanence state, the magnetic pattern splits into domains to minimize the total energy of the system (see figure 8). If we display only the measurement in the $\pm$6.5 kA m^{-1} range, we observe a sudden increase of the resistance followed by a constant region and then a decrease of the same order of magnitude. Our interpretation is that such behaviour is determined by the switching of the legs of the magnetic element. Indeed, the field values determined in our Kerr microscopy measurements match reasonably well the field interval within which the resistance has a maximum. The shape of the MR curve can be explained assuming that a multidomain pattern still exists at these values of H_{ext} and considering the symmetry of the sensor. The first switching event can be associated with a change in the magnetization distribution so that the average value of θ is closer to 0°. When the second leg switches, the magnetization distribution will be similar to the initial configuration but with an opposite average orientation of the magnetization. This explains why the magnetoresistance jumps to the value measured before the first switching. The second switch that takes place at a difference of approximately 2.4 kA m^{-1} can be attributed to the pinning of the local magnetization and probably to the interaction between the legs, especially in the upper region. The minor loop in figure 7(*c*) can also be related to the above-mentioned aspects. Considering that the magnetization in one of the legs switches at the value of 2.4 kA m^{-1} and reverses at $-$3.2 kA m^{-1} we can determine the interaction field $H_{\mathrm{I}} = 400$ A m^{-1}. We conclude that the switching of the individual legs can be observed in the MR measurements. This is important for the final sensor because we can identify this influence in the measured response.

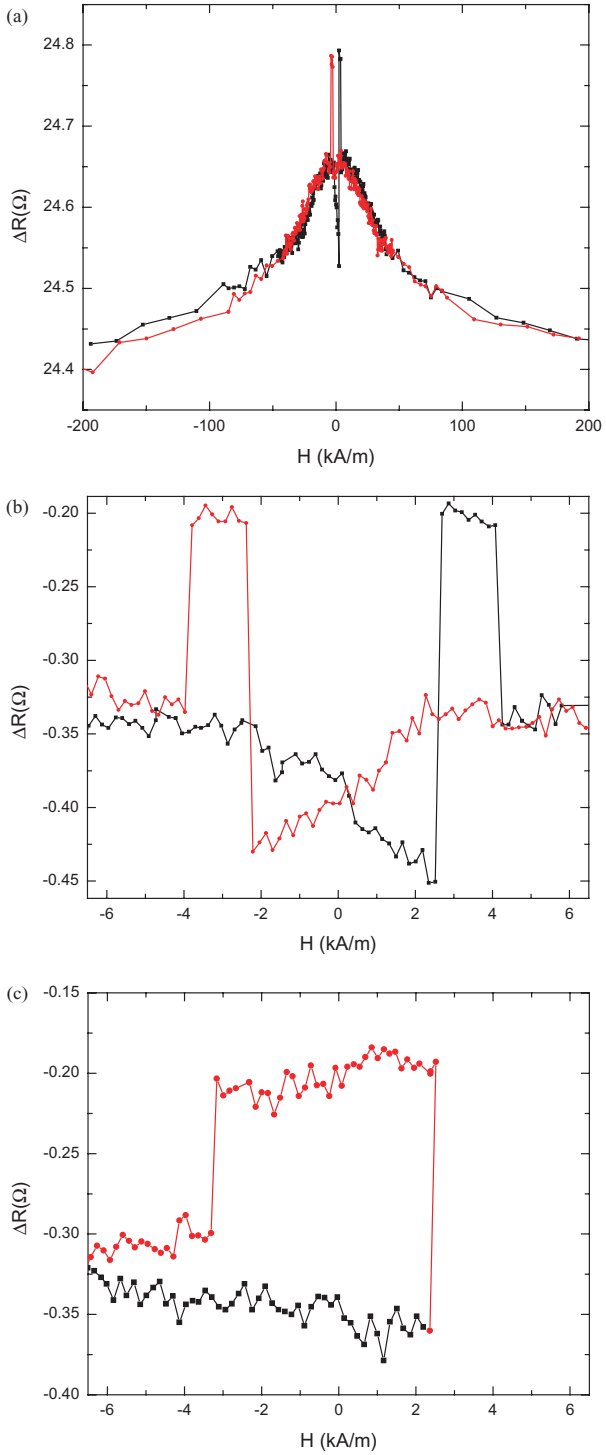

Figure 7. (*a*) DC field MR measurement of a magnetic element ($H_{\mathrm{ext}}||U$) and (*b*) a zoom in the region close to 0 A m^{-1}; (*c*) minor loop for the same geometry after the first switching. DR is the relative magnetization. (*d*) MFM scan of a sensor in the remanence state—the saturation field was parallel to the legs.

That large stray fields are created at the extremities of the sensor, can be concluded by observing the magnetic contrast at the top region in the MFM image with the region at the bottom of the structure (figure 8). The fact that we observe dark–light contrast at the extremities indicates that a charge-type sensor-MFM tip interaction is present. Yet, the

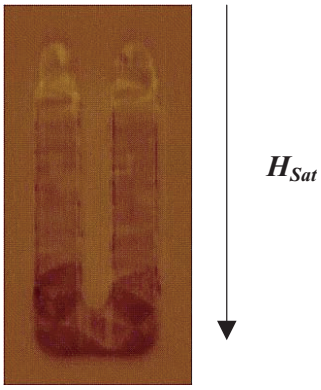

Figure 8. MFM scan of a sensor in the remanence state; the saturation field was parallel to the legs.

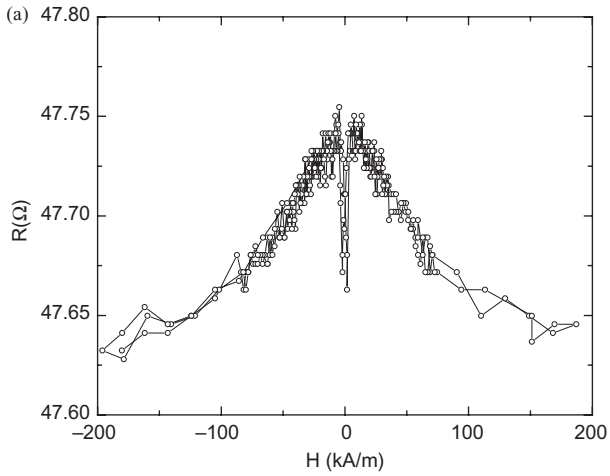

Figure 9. (*a*) MR measurement of an etched structure; (*b*) MFM image of the etched structure.

susceptibility-type contrast visible in the middle of the sensor, where all the spins are supposed to lie in the horizontal plane, can be assigned with a slight influence of the tip on the local magnetization. For more details on the interpretation of the measurements we refer to [13]. At small values of the field this image is not expected to change significantly.

The last magnetoresistance measurement (figure 9(*a*)) corresponds to the sensor presented in figure 5(*b*). As expected, the total resistance is almost double due to the trenches applied in the etching process. The changes in resistance at high fields have an origin similar to that for the structure before it was etched by FIB. We observe a fast decrease of the magnetization at small H_{ext} values, in contrast with figure 7(*b*). The magnitude of the effect is almost the same as estimated between the high field values and maximum values of the resistance. Similar to the previous situation, we may associate the resistance measured at small field values with the changes in magnetization in the sensitive area indicated in figure 9(*b*). Once again the MFM scans support the MR results. Indeed, we see that the magnetization distribution at the bottom of the sensor has a vortex-like structure. Consequently, the average angle between the local magnetization and the current direction will be close to zero. The change of this angle can be produced either by applying a local field in that area of the sensor (like from a bit pattern) or by an antiparallel orientation of the magnetization in the legs (like in previous situation). For writing purposes one must take into consideration the fact that the sensor saturates at about 160 kA m^{-1}. Therefore, the storage medium presented in section 2 will be useful if a proper stray field at the end of the sensor can be obtained in much lower fields. Further experiments will be performed in order to establish the minimum bias field that will induce a distribution of magnetization at the end region of the sensor, creating a stray field strong enough for writing purposes. The experiments will be performed by measuring the magnetoresistance in a constant field H_{ex} and simulating a bit pattern with a MFM tip.

4. Conclusions

We have proposed a new design for magnetic sensors which can be integrated in a probe array memory. The particular feature of this sensor is that it will be able to perform both writing and reading operations. We have demonstrated that probe writing in a magnetic medium can be performed in a heat-assisted process using conductive magnetic tips. In our experiments a reversal of the magnetization can be obtained on a scale as small as 130 nm. Although we have used magnetic layers evaporated on conventional AFM tips for these experiments, the integration of the sensor on a cantilever tip will enable similar performances. By designing the MR sensor using micromagnetic simulations, we have adopted a sensor shape that will determine a vortex-like magnetization distribution, which enhances the stability of the sensor. The experimental realization of a sensor with a sensitive region similar to the one suggested by the simulations, showed a measurable change in its magnetization distribution. From these preliminary experiments we conclude that the MR sensor proposed by us is suitable for integration on cantilever tips. Proper cantilevers for this purpose were already developed in our group [11] and [14].

Further improvements of the performance of the storage system can be obtained in several ways. First, we can scale down the dimensions of the sensor to increase the lateral resolution. The physical limitation is given by the strength of the exchange interactions of the magnetic material. This is because if the exchange energy is stronger than the demagnetizing energy, specific for our particular

shape, the magnetization distribution will not have a vortex-like distribution. Also, multilayer structures can be considered as candidates for reducing the signal to noise ratio of the sensor. In this respect, GMR or TMR sensors will give a much larger MR ratio. Ultimately, when the spatial resolution of the sensor is smaller than the size of the single reversed magnetic domain, one can increase the perpendicular anisotropy of the medium. In this way, we can decrease both the size of the individual reversed magnetic volumes as well as the distance between them.

References

[1] Eleftheriou E, Binning G K, Cherubini G, Despont M, Dholakia A, Durig U, Lantz M A, Pozidis H, Rothuizen H E and Vettiger P 2003 Millipede-a mems-based scanning-probe data-storage system *IEEE Trans. Magn.* **39** 938

[2] McDaniel T W, Challener W A and Sendur K 2003 Issues in heat-assisted perpendicular recording *IEEE Trans. Magn.* **39** 1972

[3] Zhang L, Bain J A and Zhu J G 2002 Dependence on thermomagnetic mark size on applied stm voltage in co–pt multilayers *IEEE Trans. Magn.* **38** 1895

[4] Mansuripur M 1998 *The Physical Principles of Magneto-Optical Recording* (Cambridge: Cambridge University Press)

[5] Meng Q, de Haan P, van Drent W P, Lodder J C and Popma Th J A 1996 *IEEE Trans. Magn.* **32** 4064

[6] Onoue T, Siekman M H, Abelmann L and Lodder J C 2003 *J. Magn. Magn. Mater.* **32** 4064

[7] Abelmann L, Kizroev S K, Litvinov D, Zhu J G, Bain A, Kryder M H, Ramstock K and Lodder C 2000 Micromagnetic simulation of an ultrasmall single-pole perpendicular write head *J. Appl. Phys.* **87** 6636

[8] Ramstock K Magfem3d program, http://www.ramstock.de/

[9] Ozkaya D, Langford L, Langford R M, Chan W L and Petford-Long A K 2002 Effect of Ga implantation on the magnetic properties of permalloy thin films *J. Appl. Phys.* **91** 9937

[10] Bae S, Judy J H, Tsu I F and Murdock E S 2001 *J. Appl. Phys.* **90** 2427

[11] van den Bos A, Heskamp I, Siekman M, Abelmann L and Lodder C 2002 *IEEE Trans. Mag.* **38** 2441

[12] Schfer R 2003 *IEEE Trans. Magn.* **39** 2098

[13] Hubert A, Rave W and Tomlinson S L 1997 Imaging magnetic charges with magnetic force microscopy *Phys. Status Solidi* b **204** 817

[14] van den Bos A 2003 Planar fabrication of probes for magnetic imaging *Thesis* University of Twente, The Netherlands